

Tribological Behavior and Corrosion Properties of Graphite Incorporated Cu/SiC Nanocomposite Coatings Prepared by Pulse Current Electrodeposition

Seyed Mahmood Mirsaeed-Ghazi¹, Saeed Reza Allahkaram¹ and Arman Molaei^{2*}

¹School of Metallurgy and Materials Engineering, University College of Engineering, University of Tehran, P.O. Box 11155-4563, Tehran, Iran

²Department of Science and Technology, Organic Electronics, Linköping University, Norrköping SE-60174, Sweden

*Corresponding author: Arman Molaei, Department of Science and Technology, Organic Electronics, Linköping University, Norrköping SE-60174, Sweden, Tel:+46 13 28 10 00; E-Mail: Arman.Molaei@yahoo.com

Received: April 10, 2018; Accepted: April 27, 2018; Published: April 30, 2018

Abstract

In this research, Cu/SiC/graphite nanocomposite coatings were fabricated by using pulse current (PC) electrodeposition method in the sulfate bath. The effects of PC parameters, like frequency, duty cycle, current density, and graphite concentration in the electrolyte bath, on the codeposition of graphite microparticles in the coating were analyzed. Also, the Cu-based composite coatings were tested by means of scanning electron microscopy (SEM) equipped with energy dispersive X-ray (EDX) spectroscopy, Vickers microhardness, and X-ray diffraction (XRD) techniques. Finally, the corrosion behavior of coatings in 3.5 wt.% NaCl solution were evaluated by using potentiodynamic polarization technique. The maximum code position of graphite was achieved at the current density of 12 A/dm², frequency of 15 Hz, duty cycle of 7%, and graphite content of 60 gr/l. Increasing graphite microparticles and decreasing SiC nanoparticles in the Cu-based composite coatings led to a decrease and increase in SiC content of the deposition, microhardness, friction coefficient, corrosion, and wear resistance, respectively. Furthermore, by embedding desirable SiC and graphite particles, Cu-based coating on the Cu substrate obtained both great wear and corrosion resistance.

Keywords: *Electrodeposition; Nanocomposite; Graphite microhardness; Tribological properties; corrosion.*

Introduction

Nowadays, Copper and Copper alloys are among the most important commercial and industrial metals ranked the third position after iron/steel and aluminum in the terms of production and consumption [1]. The extensive application of Copper in

various industries has been attributed to its good corrosion resistance, excellent electrical and thermal conductivity, and desirable plasticity and formability. Despite the abundant usages of pure Copper in various industries, the production of Copper composites has considerably increased [2,3].

Metal matrix composites (MMC) are as a new class of materials produced by the codeposition of fine polymeric or ceramic particles or both of them. MMCs have received much attention due to enhanced mechanical properties, elastic modulus, wear, and corrosion resistance.

Hard ceramic particles, such as Al_2O_3 [4-6], ZrO_2 [7,8], Si_3N_4 [9], SiC [10,11], and ZnO [12,13], have been utilized to augment the hardness of composite coatings. Although hard particles have a negative effect on the friction coefficient of coating, self-lubricant soft particles, such as PTFE [14], graphite [15,16], and MoS_2 [17], have been used to reduce the friction coefficient of the coating and to develop lubrication properties. The uniform distribution of particles in the matrix to prevent forming agglomerations is a most important parameter affecting the performance and expected properties of a composite coating [18]. Previous studies on the production of these materials have shown that oxides, carbides, and borides particles are insoluble in the Copper matrix leading to thermal stability at high temperatures [19]. Hence, the Copper composites are considered as reliable candidates for applications in which high conductivity, good mechanical properties, and wear resistance are simultaneously required [19,20].

Powder sintering, squeeze casting, composite electroforming, and sintering under ultrahigh pressure have been used in the production of composites [21]. The production of composite coatings utilizing different particles by electrodeposition technique is among the most common methods to produce composite materials. In this codeposition method, the composite coatings are obtained by adding particles into the electrolyte solution of plating bath. According to previous studies, the pulse current (PC) electrodeposition has resulted in improved morphological properties, particle distribution, grain size, hardness, and wear resistance compared to direct current (DC) electrodeposition [22].

Numerous studies have been done on the electrodeposition of Copper matrix composites. Wan et al. produced $\text{Cu}/\text{Al}_2\text{O}_3$, Cu/SiC , and Cu/ZrO_2 plated composite coatings with a higher hardness than pure Cu coatings. Their findings suggested a decrease in the hardness of Copper coating by the addition of graphite and CaF_2 particles [23]. Cu/SiC MMCs are among the most important MMC materials which have been widely studied [24-29].

SiC ceramic particles have great importance due to high strength, excellent resistance to corrosion and erosion, good mechanical and physical properties, low density and price, and their applications as semiconductors [30-32]. Graphite is used in the production of composite coatings due to desirable properties, such as self-lubrication and low thermal expansion coefficient. Copper matrix containing SiC and graphite particles is widely used as brushes, electrical contacts, and bearing materials [24-28,33,34].

The present study introduces the simultaneous codeposition plating of hard SiC nanoparticles and soft graphite microparticles in the Copper matrix to gather broad desirable properties in a noble structure. The microstructure, tribology, and corrosion

resistance of Cu/SiC/graphite coatings with different SiC and graphite contents were studied and compared. It can be expected that the optimum composite presents wide properties during application.

Experimental

Preparation of the substrate

Pure Copper (99.9%) samples of $3 \times 3 \times 0.2 \text{ cm}^3$ were mechanically polished by abrasive papers (up to grid 2500) and used as cathode. The surface of the pure Copper (99.9%) anode ($3 \times 3 \times 0.2 \text{ cm}^3$) was prepared with the abrasive paper 120 and rinsed after each electrodeposition stage. The cathodic samples were ultrasonically degreased in acetone for 10 min and then were immediately rinsed by distilled water. Then, the samples were acid pickled in 10 wt% sulfuric acid solution for 30 s to remove surface oxides and activate the surface. The samples were again rinsed with distilled water.

Bath preparation and operating conditions

The bath composition and electrodeposition process conditions have been listed in **TABLE 1**. The average sizes of SiC and graphite particles were 40 nm and 10 μm , respectively. To avoid forming agglomeration of particles in the electrolyte, the solution was stirred in the ultrasonic chamber three times, each one for 10 min. The solution was mixed with a magnetic stirrer for another 5 min between 10-min intervals. The distance between cathode and counter electrode (anode) was 20 mm. Additives like saccharine and Sodium dodecyl sulfate were used to rise the nucleation on the substrate and charge of particles, respectively [33,34]. Deposition was performed to achieve optimal peak current density, frequency, and duty cycle (D), graphite and SiC concentration in the plating bath as well as high microhardness, tribology, and corrosion properties.

Deposition parameters	Amount (pulse electrodeposition)
Copper sulfate (mol/l)	0.2
Sulfuric acid (mol/l)	0.2
SiC (g/l)	5
Graphite (g/l)	20, 40, 60, 80
Saccharin (g/l)	0.5
Sodium dodecyl sulfate (g/l)	0.3
Ph	1.5

Magnetic stirring speed (rpm)	200
Temperature (°C)	40
Peak current density (A/dm ²)	6, 12, 20, 30
Pulse frequency (Hz)	5, 15, 50, 80
Duty cycle (%)	7, 10, 15, 20

TABLE 1. The electrolyte composition and the electrodeposition parameters.

Analysis of electrodeposition

The microhardness of the samples was determined by vickers hardness tester (Amsler D-6700). For this purpose, a 100 g load with a dwell time of 10 s was used. The ultimate hardness was obtained from the average of five measurements.

Scanning electron microscopy (SEM, Camscan MV2300) and optical microscopy were used to study the surface morphology of coatings.

EDX analysis was used to measure the concentration of nanoparticles in the Cu-based coatings. The crystal structure of coatings was examined by X-ray diffraction (XRD) X'Pert PRO X-ray diffractometer, CoK_α radiation at 30 kV and 20 mA (in the angle range of 2θ=10-110°) with a scanning rate of 0.4°/min.

The tribological behavior of the samples was investigated by ball-on-disk test (AISI-52100 stainless steel ball, diameter 5 mm with a hardness of RC 65). All tests were performed under a 3 N load and a sliding speed of 0.9 m.s⁻¹ at room temperature. During the test, the friction coefficient was automatically measured. The Archard's law was used to determine the wear rate [35]. Accordingly, the wear rate (ω) is proportional to the applied pressure (p) and the wear rate (v):

$$\omega = \frac{K}{H(T)} pv \quad (1)$$

Where $H(T)$ is the microhardness (which is a function of temperature) and K is the friction coefficient. The surface of samples was investigated by optical microscopy to determine the wear mechanism.

To study the corrosion resistance of coatings, the potentiodynamic polarization test was performed in a 3.5 wt% NaCl solution by a EG&G potentiostat/galvanostat (Model 273A) apparatus with a sweeping rate of 1 mV/s, the potential range of -550 to 550 mV relative to the open circuit potential (OCP). Before testing, the samples were immersed in the solution for 20 min to

achieve a stable system and to reach the OCP. Platinum (Pt) and Ag/AgCl electrodes were used as auxiliary and reference electrodes, respectively.

Results and Discussion

The effect of PC electrodeposition parameters

The graphite concentration in the coating is under the influence of PC electrodeposition parameters shown in **FIG. 1** and 1a presents the effect of peak current density on the codeposition of graphite particles in the coating at the frequency of 80 Hz and duty cycle of 5%.

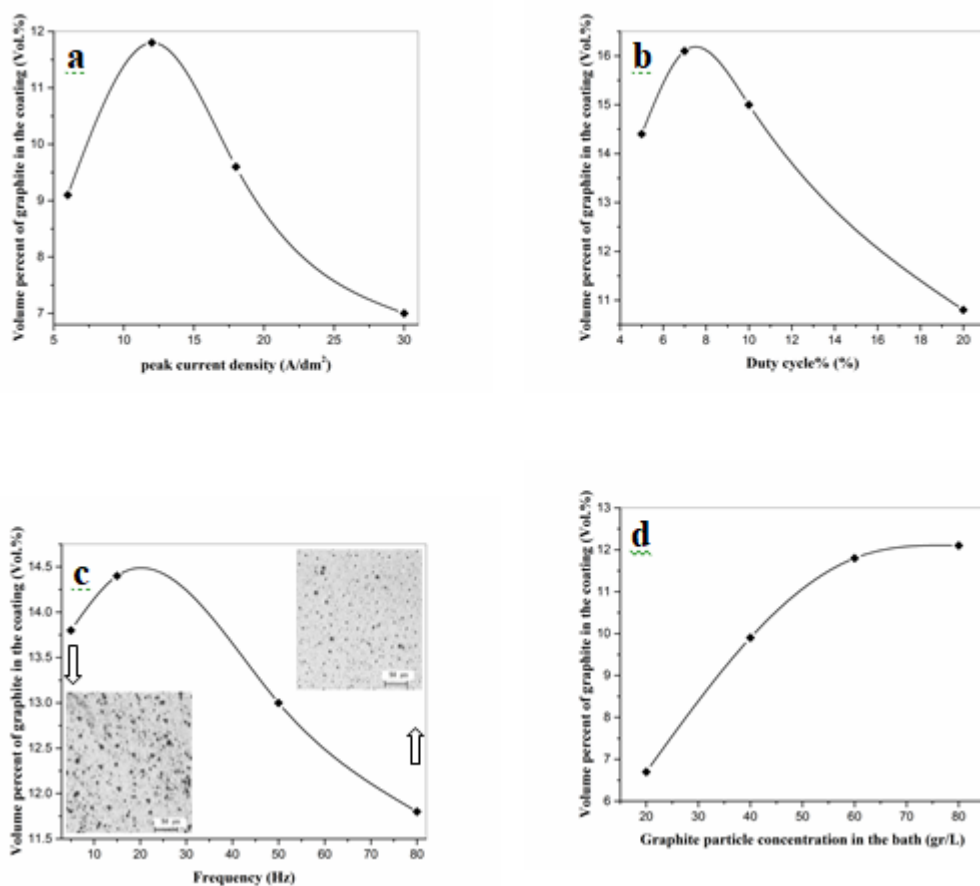


FIG. 1. The contented graphite in the coating under the influence of PC electrodeposition parameter: (a) peak current density, (b) duty cycle, (c) frequency, (d) graphite concentration.

The peak current density of 12 A/dm² presents the highest level of deposited graphite particles in the coating (FIG 1a). It is perceivable that the deposition rate of graphite particles decreases by changing the current density than this value (12 A/dm²).

In the electrolyte solution, the Cu^{2+} ions as well as SiC and graphite particles move towards the cathode under the stirring and electrophoretic movements due to the solution agitation and applied potential, respectively. In the present case, these two factors do not act independently. Instead, they affect each other and the resulting movement of the Cu^{2+} ions and nanoparticles are decided by their individual action at any particular moment.

At low peak current density (i.e. 6 A/dm^2), there is no strong electric field to obtain a high electrophoretic force for pushing graphite microparticles towards the cathode. Thus, a lower amount of graphite reach to the cathode surface and incorporate into the deposition. While applying the current density of 12 A/dm^2 results in improving the electrophoretic movement and moving graphite microparticles in the electrolyte bath and depositing.

By increasing more than 12 A/dm^2 , due to the more mobility of ions rather than that of particles, the deposition rate of metal ions is a higher amount than that of particles. Therefore, it is expectable that in a higher amount of current density, most of the ions lonely move towards the cathode instead of surrounding around particles (electrophoretic movement). Therefore, the deposition rate of graphite microparticles reduces.

The volume percent of the deposited graphite particles in the composite coating as a function of the duty cycle is shown in **FIG. 1b** at the peak current density of 12 A/dm^2 and frequency of 15 Hz .

It is observable from **FIG. 1b**, more graphite deposits, by increasing the duty cycle from 5% to 7% and then by rising more, the graphite deposition decreases.

By the enhancement in the duty cycle from 5% to 7%, according to Eq. 2, more pulse width (PW), i.e. higher pulse active time, is achieved in the total period of the signal (T).

$$D = \frac{PW}{T} \times 100 \quad (2)$$

In this circumstance, graphite microparticles have more time for moving and incorporating in the deposition.

Moreover, as it is verified, during OFF-time (T_{OFF}), ions and particles compete in the same conditions [36]. This behavior augments the chance of particles to present nearby cathode and deposit at the cathode surface by applying voltage. At the duty

cycle range of 5% to 7%, there is high T_{OFF} and subsequently more probability to deposit graphite particles on the cathode. Therefore, in regards to two mentioned phenomena, with the enhancement of duty cycle from 5% to 7%, more graphite particles deposite on the cathode surface.

While, the deposition of graphite microparticles decreases by rising duty cycle from 7% to 20%. It demonstrates the effect of high mobility of free ions than ones of the ceramic particles. By increasing duty cycle, i.e. more the ON-time (T_{ON}), due to a higher mobility of Cu^{2+} ions than those of ceramic particles, the deposition of graphite particles reduces. Furthermore, owing to short T_{OFF} , charging of graphite microparticles around the cathode surface has a low probability.

Totally, with an increase of the duty cycle from 7% to 20%, a lower magnitude of graphite microparticles incorporates into the composite coating.

Frequency has a significant effect on T_{ON} and T_{OFF} as well as the distribution of particles in coatings [37]. **FIG. 1c** shows the effect of pulse frequency on the volume percent of deposited graphite particles in the nanocomposite coating at peak current density of 12 A/dm² and duty cycle of 7%. The graphite microparticles incorporated into the Cu-SiC coating is also analyzed by SEM depicts in **FIG. 1c**.

As seen in **FIG. 1c**, the maximum and minimum concentration of graphite particles in the coating is obtained at the frequency of 15 Hz and 80 Hz, respectively. Changing frequency from this value achieves composites with a lower presence of graphite incorporation. This behavior can be explained as follows.

At low frequency, the charging time is much shorter than T_{ON} , and the time is required for the discharge of the double layer is much shorter than T_{OFF} between two pulses. At the frequency lower than 15 Hz, owing to the short charging time and consequent incomplete charge of Cu ions adsorbed on graphites, the minimum number of graphite microparticles incorporates into the nanocomposite coating. Therefore, a low graphite percent presents into the Cu matrix.

At high frequency, charging and discharging times of the double layer are much longer than T_{ON} and T_{OFF} of the pulse, respectively, and the pulse current virtually changes to a direct current (capacitance effect), and losing the potential advantages of pulse plating in terms of changes in the electrodeposited structure. At the higher frequency from 15 Hz, because

of the capacitance effect and consequent incomplete discharge of ions adsorbed on graphite particles, the graphite content of the coating diminishes (**FIG. 1c**). In addition, the T_{OFF} is too short to remove the concentration gradient of graphite microparticles adjacent to the cathode surface leading to the decreasing in the content of the embedded microparticles in the coating. Thus, at high frequencies, a low graphite percent achieves.

The structure of nanocomposite coating fabricated at the frequency of 15 Hz, studied by SEM, and shows in **FIG. 1c**. It is obvious that the maximum dispersed SiC content in the nanocomposite coating is obtained. That is because of the moderate T_{ON} and T_{OFF} that are approximately equal to the charging and discharging times of Cu^{2+} ions on graphite microparticles. Thus, Cu-SiC nanocomposite coating prepared at the frequency of 15 Hz has a most presence of graphite microparticles.

FIG. 1d illustrates the effect of contented graphite concentration in the bath on its deposition in the Cu-SiC coating at the peak current density of $12 A/dm^2$, frequency of 15 Hz, and duty cycle of 7%.

By the addition of more graphite concentration in the plating bath, the volume percent of deposited graphite microparticles increases until reaching a constant level (**FIG. 1d**).

The effect of graphite concentration contained in the electrolyte solution on Cu-based deposition follows a Langmuir isotherm adsorption phenomenon [38]. Rising the concentration in the solution causes the enhanced flux of microparticles toward the cathode and consequently more number of graphites reach the cathode surface. During deposition, only the particles that have enough time to attach the cathode surface are likely to be deposited. In this circumstance, trapping of graphite particles in the growing metal matrix is dependent on the deposition rate relating to the Cu metal, SiC nanoparticles, and graphite microparticles.

By increasing the concentration of graphite, the deposition reaches a maximum value, equilibrium value (**FIG. 1d**). The equilibrium condition occurs when the number of deposited particles is equal to the number of particles reached the cathode surface. In this condition, by increasing the concentration of graphite particles than the saturation concentration, the graphite particles are more likely to be agglomerated. Agglomerated graphites show a resistance against deposition and act as a barrier against the flux of SiC nanoparticles entering the cathode. Therefore, the volume percent of graphites deposited in the Cu matrix may be diminished. Due to the trapping capacity of growing metal remains unchanged, graphite particles are not

agglomerated consequently, the co-deposition rate becomes constant after a certain concentration.

FIG. 2. It studies the microhardness of composite coating fabricated by PC electrodeposition. **FIG. 2a** depicts the effect of graphite concentration in the plating bath on the SiC content in the composite coatings.

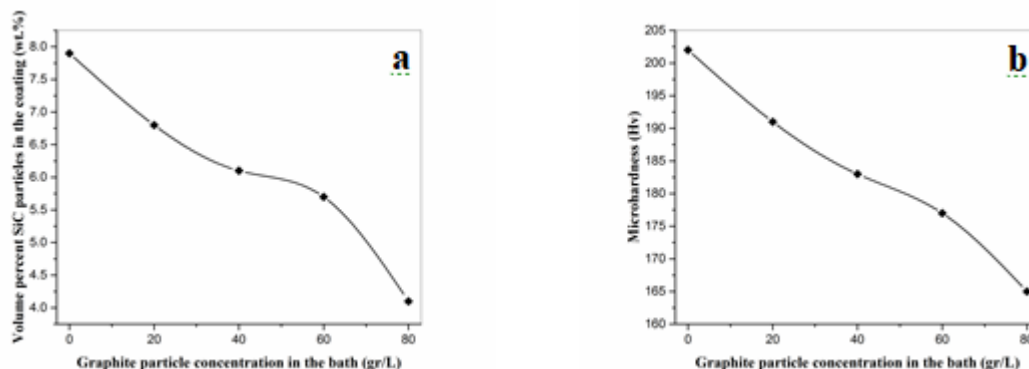


FIG. 2. Effect of graphite concentration in the plating bath on (a) the SiC concentration and (b) microhardness of the composite coatings at the constant peak current density of 12 A/dm², frequency of 15 Hz, and duty cycle of 7%.

As it is obvious in **FIG. 2a**, a decreasing SiC concentration yields by increasing the graphite content in the coating. The reason of this behavior is that the graphite particles in the electrolyte solution act as a barrier against of the SiC particles and prevent them from reaching to the cathodic electrode. It is partially contribute to the trapping capacity leading to a reduction in the concentration of SiC particles in the coating. This is intensified at high concentration of graphite where the probability of agglomeration and the creation of a barrier on the path of ceramic particles is more probable.

FIG. 2b shows the effect of contented graphite particles in the bath on the microhardness of yielded coating.

It is observable that rising the concentration of graphite in the electrolyte solution leads to a reduction in the microhardness of Cu-based composite coating (**FIG. 2b**). The reduction in the microhardness of the coating can be explained in the following phenomena.

First, the graphite particles deposited in the coating have a low microhardness leading to a decrease in the hardness of composite coating. Second, the graphite particles in the electrolyte solution prevent the hard SiC particles from reaching to the cathode (**FIG. 2a**). Third, the microsized graphite particles occupy high volume in the composite coating.

Coating Characterization

Morphological and structural study

The surface morphology of the Cu-5.7% SiC and Cu-5.7% SiC-11.8% graphite composite coatings are analyzed by SEM, presents in **FIG. 3a** and **b**.

By comparing **FIG. 3a** and **b**, the addition of 60 g/l graphite in the nanocomposite coating incorporates graphite particles in the Cu-SiC coating. Also, it is demonstrable that the deposition of graphite microparticles prevents from depositing SiC nanoparticles at the cathode surface.

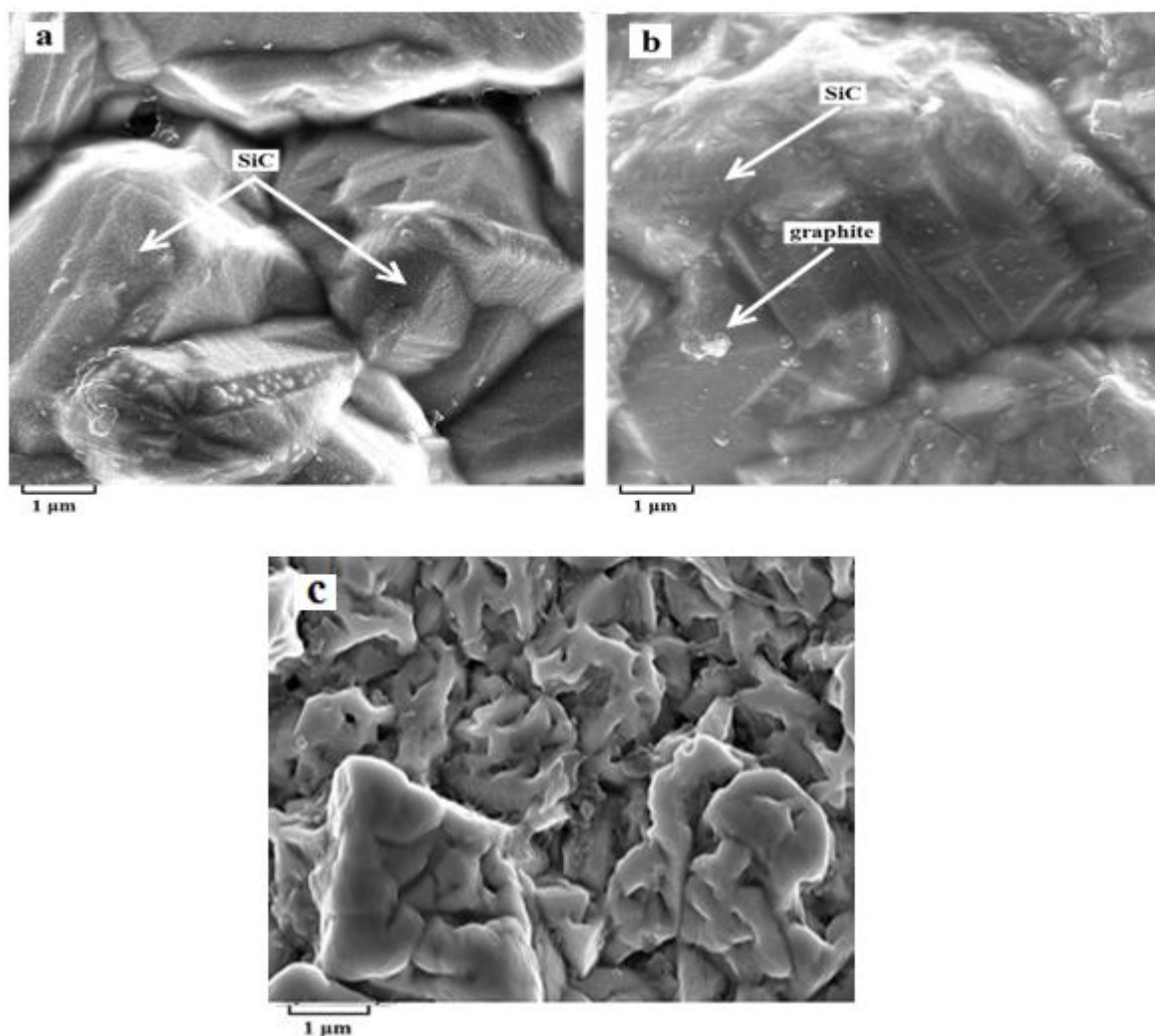


FIG. 3. Surface morphology SEM images of the composite coatings fabricated in the plating bath containing (a) 5.7 g/l SiC without graphite and (b) with 60 g/l graphite at the peak current density of 12 A/dm², frequency of 15 Hz, and duty cycle of 7% and (c) the peak current density of 12 A/dm², frequency of 80 Hz, and duty cycle of 5%.

The simultaneous effect of the frequency and duty cycle is evident by comparing FIG. 3b and c. A more frequency and lower duty cycle, owing to the reduction of the concentration polarization and subsequently increase of the current density, a more uniform coating fabricates with a lower grain size (FIG. 3c). Furthermore, in regard to these changes, a lower graphite contents achieves in the Cu-based coating.

X-ray diffraction studies also indicate that the growth orientation of Copper crystals during the plating process changes with simultaneous addition of SiC and graphite particles from the (1 1 1) plane for the pure Copper (FIG. 4a) to (0 0 2) plane for the Cu-6.8% SiC-6.7% graphite coating (FIG. 4b).

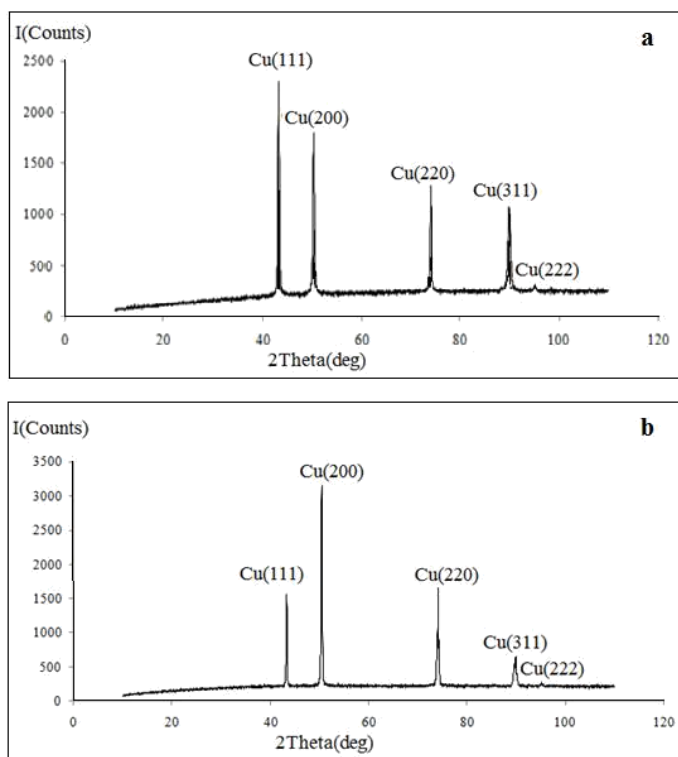


FIG. 4. XRD pattern of (a) pure Cu and (b) Cu-6.8% SiC-6.7% graphite coating at the constant peak current density of 12 A/dm², frequency of 15 Hz, and duty cycle of 7%.

More interestingly, by the addition of particles in the electrolyte bath, larger peaks and subsequently a lower grain size observes. The presence of particles in the electrolyte solution and subsequently at the surface of the cathode provides the

nucleation sites for the electrocrystallization leading to increased nucleation and reduced crystallite size following a higher microhardness.

Friction and wear analyses

Variation of the friction coefficient of Cu-7.9% SiC and Cu-4.8% SiC-16.1% graphite composite coatings tested to a 100 m sliding distance represents in **FIG. 5**.

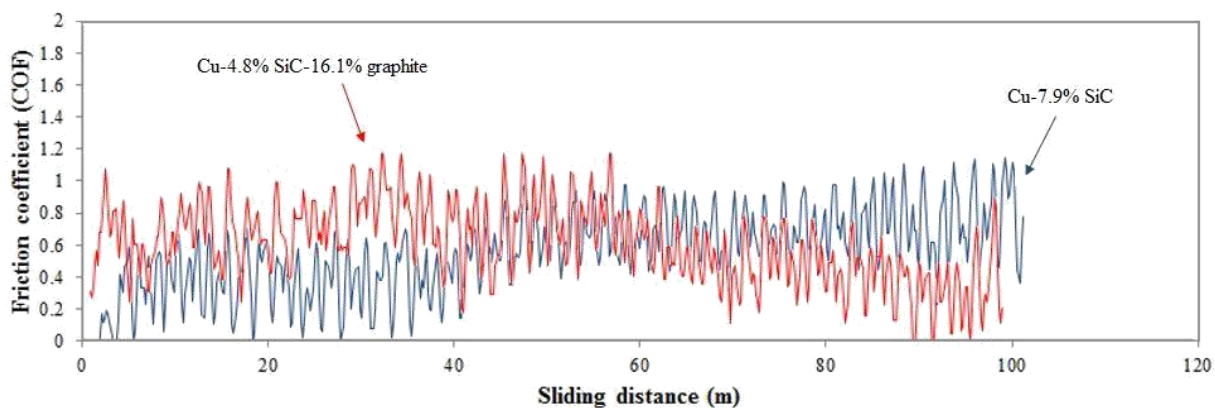


FIG. 5. The comparison of friction coefficients between Cu-7.9% SiC and Cu-4.8% SiC-16.1% graphite composite coatings as a function of sliding distance.

As it is obvious, more friction coefficient achieves by increasing the concentration of graphite in the composite coating. Also, owing to more SiC content in the Cu-7.9% SiC composite coating, tribological analysis exhibits more friction resistance. **FIG. 6** illustrates the friction coefficient of Cu-SiC coatings containing the graphite concentrations of 0, 6.7, 11.8, and 16.1 wt. %. The average values relating to the friction coefficient imply that with increasing and decreasing the graphite and SiC concentrations, respectively, the friction coefficient of coating reduces. The minimum friction coefficient observes for the coating with a graphite concentration as much as 16.1 vol%.

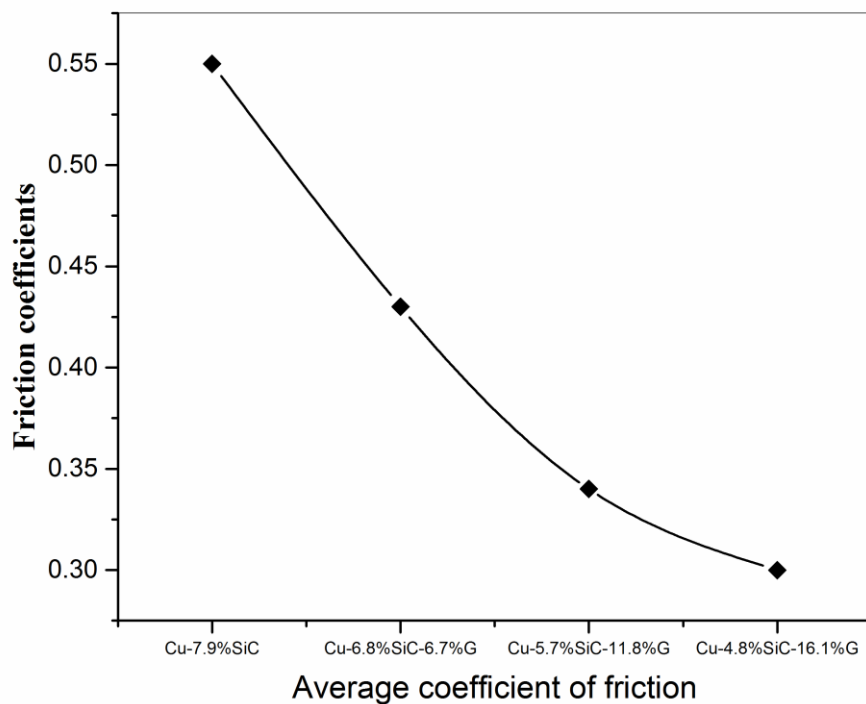


FIG. 6. Effect of graphite content in deposition (wt. %) on the friction coefficient of composite coatings.

The results of **FIG. 6** are relating to the formation of a graphite layer on the surface during the erosion process and thereby the separation of pin and sample surface at the microscopic level and subsequently reduced adhesion. Since graphite has a layered structure, the graphite layers can easily slide on each other. Therefore, a shear stress is exerted to this weak graphite layer leading to easier slide of the pin on disk. Moreover, because of the decrease in the SiC incorporation in the coating has an important effect on the declining trend of curve. This fact results from the reduction of contact between pin and Cu matrix coating.

As it can be seen in **FIG. 7**, in pin-on-disk test, the weight loss of samples is also measured.

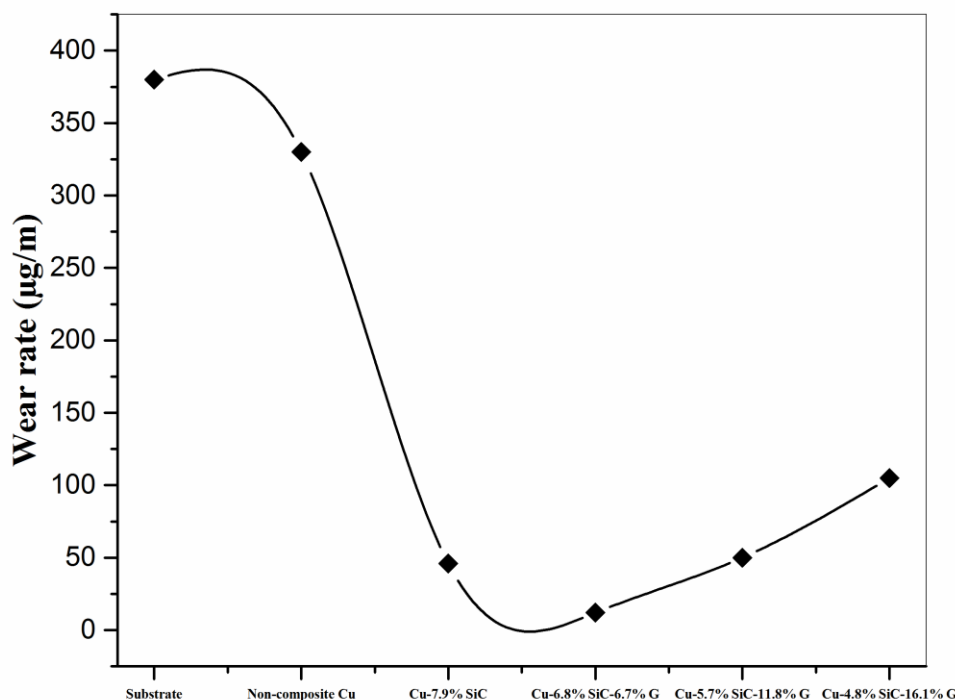


FIG. 7. The wear rate of substrate, non-composite Cu, Cu-7.9% SiC, Cu-6.8% SiC-6.7%graphite, Cu-5.7% SiC-11.8% graphite, and Cu-4.8% SiC-16.1% graphite.

It is distinguishable from FIG. 7, Cu substrate has a minimum wear rate, i.e. a maximum wear resistance (380 µg/mm). With the formation of the noncomposite coating, the wear rate declines to 330 µg/mm. Embedding 7.9% SiC in the noncomposite coating results in significantly reducing the wear rate to 46 µg/mm. Also, slightly increasing trend of curve pertaining to the incorporation of lower and higher SiC and graphite particles in the nanocomposite coating, respectively.

Owing to the fabrication of Cu coating with different structures and morphologies, the wear rate is analyzed in a lower value. The decreasing effect of SiC nanoparticles on the wear rate can be the result of augmenting the hardness of the nanocomposite coatings, improving bonding between Cu matrix and SiC nanoparticles, and reducing in the direct load contact between the Cu-SiC nanocomposite surface and disk.

The presence of graphite particles in the composite coating prepared by the pulse method increases the relative wear rate

because of the following reasons:

- I. The enhancement of lubrication properties and the reduction of hardness relating to the composite coating.
- II. The decrease of adhesion between the pin and disc.
- III. The reduction of deposited SiC particles and thereby the decrease of hardness since graphite particles have a lack of enough strength and the bond between its atoms. FIG. 8 tests the wear behavior of Cu-SiC/graphite coating by changing the concentration of SiC and graphite.

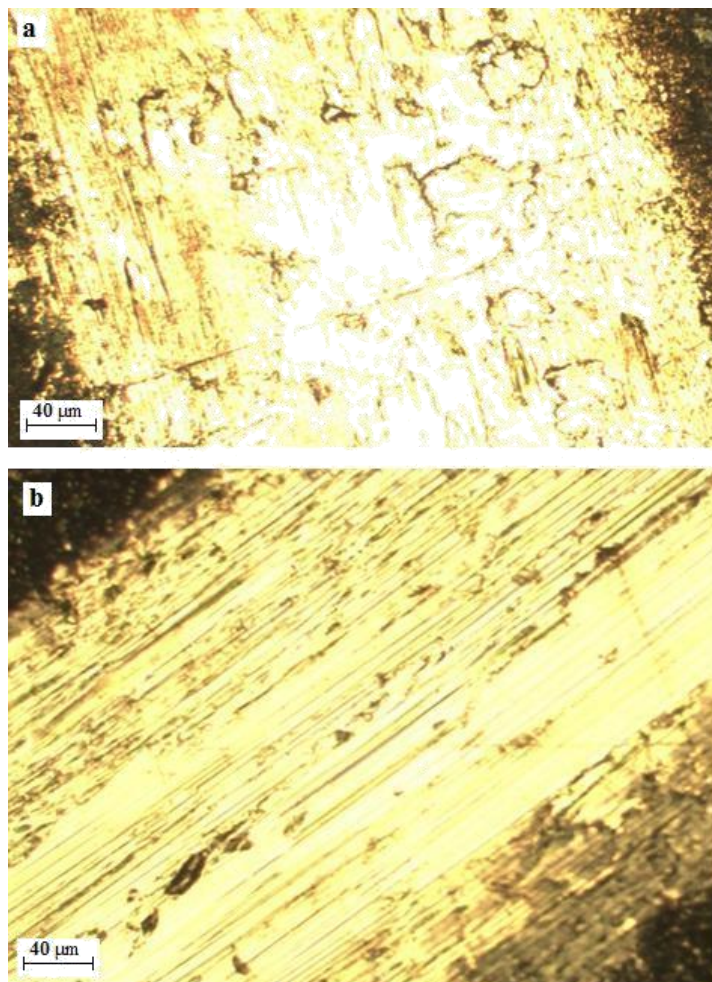


FIG. 8. Optical image of surface (a) Cu-7.9% SiC and (b) Cu-6.8% SiC-6.7% graphite.

FIG. 8a shows the optical microscope micrograph of the surface of Cu-7.9% SiC coating. The plastic deformation associating to the scratches is evident. Thereby, the wear behavior of the graphite-free coating is adhesive wear type. However, the presence of parallel scratch lines along the wear track is a sign of abrasive wear mechanism. According to the wear track and

scratches in the Cu-6.8% SiC-6.7% graphite coating, it can be concluded that the adhesion between the two surfaces is reduced in the presence of lower SiC and higher graphite particles (**FIG. 8b**).

Corrosion behavior

Potentiodynamic polarization curves for the Cu substrate, Cu-SiC/graphite composite coatings in 3.5% sodium chloride solution presents in **FIG. 9**. The corrosion potential (E_{corr}), corrosion current density (i_{corr}), and corrosion rate are summarized in **TABLE 2**.

Samples	i_{corr} ($\mu\text{A.cm}^{-2}$)	E_{corr} (mv)	Corrosion rate (mpy)
Bare Cu substrate	10	-250	4.58
Cu/6.3% SiC	3	-250	1.38
Cu/7.9% SiC	0.9	-190	0.41
Cu/6.8% SiC-6.7% graphite	1.5	-230	0.69
Cu/5.7% SiC-11.8% graphite	7.5	-285	3.45
Cu/4.8% SiC-16.1% graphite	8	-280	3.68

TABLE 2. Corrosion potential (E_{corr}), corrosion current (i_{corr}) and corrosion rate of substrate and Cu/SiC/graphite composite coatings.

According to the results, the corrosion rates of all coatings are lower than that of the Copper substrate. By the addition of SiC nanoparticles in the plating bath, The E_{corr} and I_{corr} of the Cu-SiC composite coating increases and decreases, respectively. While, the addition of graphite microparticles decreases and increases E_{corr} and I_{corr} , respectively. Also, The addition of SiC and graphite particles to this coating decreased and increased the corrosion rate.

The incorporation and distribution of SiC nanoparticles fill active corrosion sites, surface defects, and holes and block, thereby decrease anodic and cathodic reactions. Furthermore, the presence of SiC nanoparticles reduces the contact surface of the corrosive environment with the substrate. Both reactions result in reducing the level of contact with the corrosive environment and consequently increasing the corrosion resistance.

Moreover, the increased micrographite concentration not only decreases the chance of SiC nanoparticles to be trapped in the coating, but also it reduces the surface compaction of the coating. Reduced surface compaction and increased porosity allow a

greater penetration of chloride ions and increased effective area of corrosion.

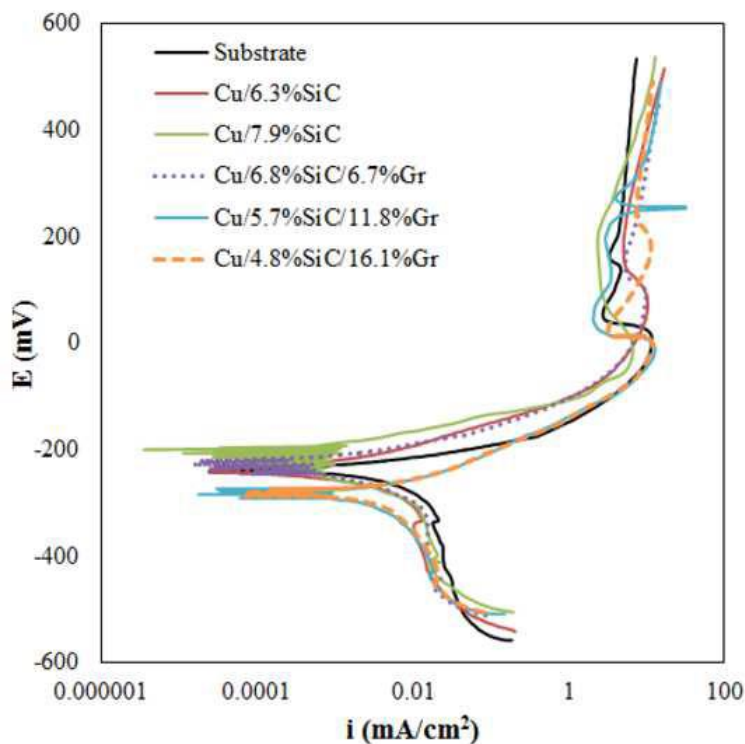


FIG. 9. Potentiodynamic polarization curves for Cu substrate, Cu-6.3% SiC, Cu-7.9% SiC, Cu-6.8% SiC-6.7% graphite, Cu-5.7% SiC-11.8% graphite, and Cu-4.8% SiC-16.1% graphite nanocomposite coatings.

As it is illustrable from FIG. 9 that Cu-SiC coating with 7.9 vol% SiC content depicts the highest corrosion resistance among the samples. The corrosion rate of this coating is 11 times lower than that of the Copper substrate.

Conclusions

In this work, the Cu/SiC/graphite composite coatings were deposited by PC electrodeposition technique on the Copper substrate. Pulse current electrodeposition parameters such as peak current density, pulse frequency, duty cycle, and graphite concentration in the electrolyte bath affect the codeposition of graphite in the prepared composite coating. The following points indicating the main findings of the present study:

1. The incorporation of graphite particles in the Cu/SiC/graphite coating experienced an enhancement with increasing the current density from 6 to 12 A/dm² and then fall with increasing the current density above 12 A/dm².
2. The most co-deposition rate of graphite particles was observed at the frequency of 15 Hz and duty cycle of 7%.

3. The concentration of graphite particles in the coating increased with rising the graphite concentration in the plating bath. The increase of graphite concentration in the bath above 60 g/l resulted in little change in graphite content in the coating.
4. Increased concentration of graphite and competition with SiC for deposition reduced the codeposited SiC particles and thereby reduced the microhardness of the coating.
5. By rising the concentration of graphite particles in the coating, the friction coefficient decreased.
6. The addition of graphite particles to the Cu/SiC composite coating reduced the wear rate while increasing the graphite particles led to an increase in the wear rate.
7. The maximum corrosion resistance was observed for the Cu/7.9% SiC coating. The addition of SiC and graphite particles to this coating decreased and increased the corrosion rate.

References

1. Efe GC, Ipek M, S. Zeytin, et al. An investigation of the effect of SiC particle size on Cu–SiC composites. *Compos part B engg.* 2012;43:1813-22.
2. Pradhan AK, Das S, Pulse-reverse electrodeposition of Cu–SiC nanocomposite coating: Effect of concentration of SiC in the electrolyte. *J Alloys Compd.* 2014;590:294-302.
3. Li X, Wang X, Gao R, et al. Study of deposition patterns of plating layers in SiC/Cu composites by electro-brush plating. *Appl Surf Sci.* 2011;257:10294-99.
4. Li C, Wang Y, Pan Z, Wear resistance enhancement of electroless nanocomposite coatings via incorporation of alumina nanoparticles prepared by milling. *Mater Des.* 2013;47:443-8.
5. Chen X, Zhang P, Wei D, et al. Tribological Behavior of Aluminum Slurry Coating on 300M Steel. *J Mater Eng Perform.* 2017;26:3719-27.
6. Balaraju J, Rajam K, Electroless ternary Ni–W–P alloys containing micron size Al₂O₃ particles. *Surf Coat Technol.* 2010;205:575-81.
7. Elńska KZ, Stankiewicz A, Szczygł I, Electroless deposition of Ni–P–nano-ZrO₂ composite coatings in the presence of various types of surfactants. *J Colloid Interface Sci.* 2012;377:362-7.
8. Francesco MP, Iommetti PR, Raffaelli L, An overview of zirconia ceramics: basic properties and clinical applications. *J Dent.* 2007;35:819-26.
9. Robin, Santana JCP, Sartori AF, Co-electrodeposition and characterization of Cu–Si₃N₄ composite coatings, *Surf. Coat. Technol.* 2011;205:4596-4601.
10. Allahkaram SR, Nazari MH, Mamaghani S, et al. Characterization and corrosion behavior of electroless Ni–P/nano-SiC coating inside the CO₂ containing media in the presence of acetic acid. *Mater Des* 2011;32:750-5.
11. Zhang S, Han K, Cheng L, The effect of SiC particles added in electroless Ni–P plating solution on the properties of composite coatings. *Surf Coat Technol.* 2008;202:280-7.
12. Hamid ZA, Aal AA, Hassan H, et al. Process and performance of hot dip zinc coatings containing ZnO and Ni–P under layers as barrier protection. *Appl Surf Sci.* 2010;256:4166-70.

13. Gupta TK, Application of zinc oxide varistors. *J Am Ceram Soc.* 1990;73:1817-40.
14. Zhao Q, Liu Y, Müller-Steinhagen H, et al. Graded Ni–P–PTFE coatings and their potential application. *Surf Coat Technol.* 2002;155:279-84.
15. Wu YT, Lei L, Shen B et al. Investigation in electroless Ni–P–Cg(graphite)–SiC composite coating. *Surf Coat Technol.* 2006;201:441-5.
16. Chen L, Yu G, Chu Y, et al. Effect of three types of surfactants on fabrication of Cu-coated graphite powders. *Adv Powder Technol.* 2013;24:281-7.
17. Hozer L, Jonq-Ren L, Yet-Ming, et al. Reaction-infiltrated, net-shape SiC composites. *Mater SciEng C.* 1995;195:131-43.
18. Buchner P, LÜTzenkirchen-Hecht D, Strehblow HH et al. Production and characterization of nanosized Cu/O/SiC composite particles in a thermal rf plasma reactor. *J Mater Sci.* 1999;34:925-31.
19. Efe GC, S Zeytin, CBindal, The effect of SiC particle size on the properties of Cu–SiC composites. *Mater Des.* 1980-2015;36:633-9.
20. Jia ZH, Zhao P, Ni J, et al. The Electrical conductivities and Tribological properties of Vacuum Hot-Pressed Cu/Reduced Graphene Oxide Composite. *J Mater Eng Perform.* 2017;26:4434-1.
21. Barmouz M, Givi MKB, Fabrication of in situ Cu/SiC composites using multi-pass friction stir processing: Evaluation of microstructural, porosity, mechanical and electrical behavior. *Compos part Aengg.* 2011;42:1445-53.
22. Molaei A, Yari M, Afshar MR, Investigation of halloysite nanotube content on electrophoretic deposition (EPD) of chitosan-bioglass-hydroxyapatite-halloysite nanotube nanocomposites films in surface engineering. *Appl Clay Sci.* 2016;135:75-81.
23. Wan YZ, Wang YL, Tao HM, et al. Preparation and Characterization of Different Particles–Copper Electrocomposites, *J Mater SciLett.* 1998;17:1251-3.
24. Zhu J, Liu L, Zhao H, et al. Microstructure and performance of electroformed Cu/nano-SiC composite. *Mater Des.* 2007;28:1958-62.
25. Molaei A, Yousefpour MA, Electrophoretic deposition of chitosan–bioglass–hydroxyapatite–halloysite nanotube composite coating. *Rare Met.* 2018.
26. Ramesh CS, Ahmed RN, Mujeebu MA, et al. Development and performance analysis of novel cast Copper–SiC–Gr hybrid composites. *Mater Des.* 2009;30:1957-65.
27. Zhang G, Wei ZH, Chen B, et al. Abnormal Transient Liquid Phase Bondability of High-Volume Fraction SiC Particle-Reinforced A356 Composite for Cu Interlayer and the Interlayer Improvement Routes. *J Mater Eng Perform.* 2017;26:5921-37.
28. Xing H, Cao X, Hu W, et al. Interfacial reactions in 3D-SiC network reinforced Cu-matrix composites prepared by squeeze casting. *Mater Lett.* 2005;59:1563-66.
29. Akbarpour MR, Salahi E, Hesari FA, et al. Microstructure and compressibility of SiC nanoparticles reinforced Cu nanocomposite powders processed by high energy mechanical milling. *Ceram Int.* 2014;40:951-60.
30. Molaei A, Yari M, Afshar MR, Modification of electrophoretic deposition of chitosan–bioactive glass–hydroxyapatite nanocomposite coatings for orthopedic applications by changing voltage and deposition time. *Ceram Int.* 2015;41:14537-44.

31. Faraji S, Rahim, N. Mohamed, and C. Sipaut, Effect of SiC on the corrosion resistance of electroless Cu–P–SiC composite coating. *J Coat Technol Res.* 2015; 9:115-24.
32. Zhang R, Lian G, Jingkun G, Preparation and characterization of coated nanoscale Cu/SiCp composite particles. *Ceram Int.* 2004;30:401-4.
33. Samal CP, Parihar JS, Chaira D, The effect of milling and sintering techniques on mechanical properties of Cu–graphite metal matrix composite prepared by powder metallurgy route. *J Alloys Compd.* 2013;569:95-101.
34. Molaei A, Amadeh AA, Yari M, et al. Structure, apatite inducing ability, and corrosion behavior of chitosan/halloysite nanotube coatings prepared by electrophoretic deposition on titanium substrate. *Mater SciEngg C.* 2016;59:740-47.
35. González B, Martín A, Llorca J, et al. Numerical analysis of pin on disc tests on Al–Li/SiC composites. *J Rodríguez Wear.* 2005;259:609-12.
36. Stojak JL, Talbot JB, Investigation of electrocodeposition using a rotating cylinder electrode. *J Electrochem Soc.* 1999;146:4504-13.
37. Lajevardi S, Shahrabi T, Effects of pulse electrodeposition parameters on the properties of Ni–TiO₂ nanocomposite coatings. *Appl Surf Sci.* 2010;256:6775-81.
38. Hovestad A, Janssen LJ, Electroplating of Metal Matrix Composites by Codeposition of Suspended Particles. *Modern Aspects of Electrochemistry.* 2005;475-532.
39. Aruna ST, Bindu CN, Selvi VE, et al. Synthesis and properties of electrodeposited Ni/ceria nanocomposite coatings. *Surf Coat Technol.* 2006;200:6871-80.